Unstable manifolds computation for the 2-D plane Poiseuille flow

Pablo S. Casas[1] Àngel Jorba[2]

Abstract

We follow the unstable manifold of periodic and quasi-periodic solutions for the Poiseuille problem, using two formulations: holding constant flux or mean pressure gradient. By means of a numerical integrator of the Navier-Stokes equations, we let the fluid evolve from a perturbed unstable solution. We detect several connections among different configurations of the flow such as laminar, periodic, quasi-periodic with 2 or 3 basic frequencies and more complex sets that we have not been able to classify.

Introduction

In this work we study some aspects of the dynamics of the plane Poiseuille problem in dimension 2, in what refers to the connection among different configurations of the flow. The fluid is confined in a channel of plane parallel walls. The problem (see [1]) is modeled by the incompressible Navier-Stokes equations

$$\frac{\partial \mathbf{u}}{\partial t} + (\mathbf{u}\cdot\nabla)\mathbf{u} = -\nabla p + \frac{1}{Re}\Delta\mathbf{u}, \qquad \nabla\cdot\mathbf{u} = 0, \tag{1}$$

together with no-slip and periodic boundary conditions

$$\left.\begin{aligned} u(x,\pm1,t) = v(x,\pm1,t) = 0 \\ (u,v,p')(x+L,y,t) = (u,v,p')(x,y,t) \end{aligned}\right\} \qquad x\in\mathbb{R}, \quad y\in[-1,1], \quad t\geq 0,$$

being Re the Reynolds number, $p' = p + 2x/Re$ and $L = 2\pi/\alpha$ (α is the parameter wave number). We have considered two different formulations to drive the fluid through the channel: holding constant the total flux or the mean pressure gradient. For each of them we obtain a different definition of $Re = hU_c/\nu$, where h represents half of the channel length, U_c the velocity of the laminar flow in the centre of the channel, and ν the kinematic viscosity. To be precise

$$Re_Q = \frac{3Q}{4\nu}, \qquad Re_p = \frac{Gh^3\rho}{2\mu^2},$$

corresponds to the Reynolds numbers when we keep Q as a constant flux or G as a constant mean pressure gradient respectively. The fluid is supposed of constant density ρ and viscosity μ. The numerical approximation is detailed in [1]. Roughly, it employs Fourier and Chebyshev spectral discretizations of velocities and pressure in the periodic and transversal directions respectively. The temporal variable is approximated by means of finite differences.

In figures 1 and 2 we represent bifurcating curves of periodic and quasi-periodic flows obtained numerically in [1] using $N = 8$ and $M = 70$ spectral modes in the x and y spatial directions respectively. For the temporal discretizacion the time step has been prescribed to $\Delta t = 0.02$. Each point of those curves corresponds to the amplitude A (distance to the laminar flow in L_2-norm) of the flow (periodic or quasi-periodic) for the given value of Re. It is also marked on the curves the different stability regions, together with several Hopf bifurcations. In figure 2 at Re_{Q1}, the Hopf bifurcation of periodic flows give rise to a family of quasi-periodic solutions, whose stability is also presented. The main load of the computations has been carried out in parallel in a Beowulf cluster of PCs.

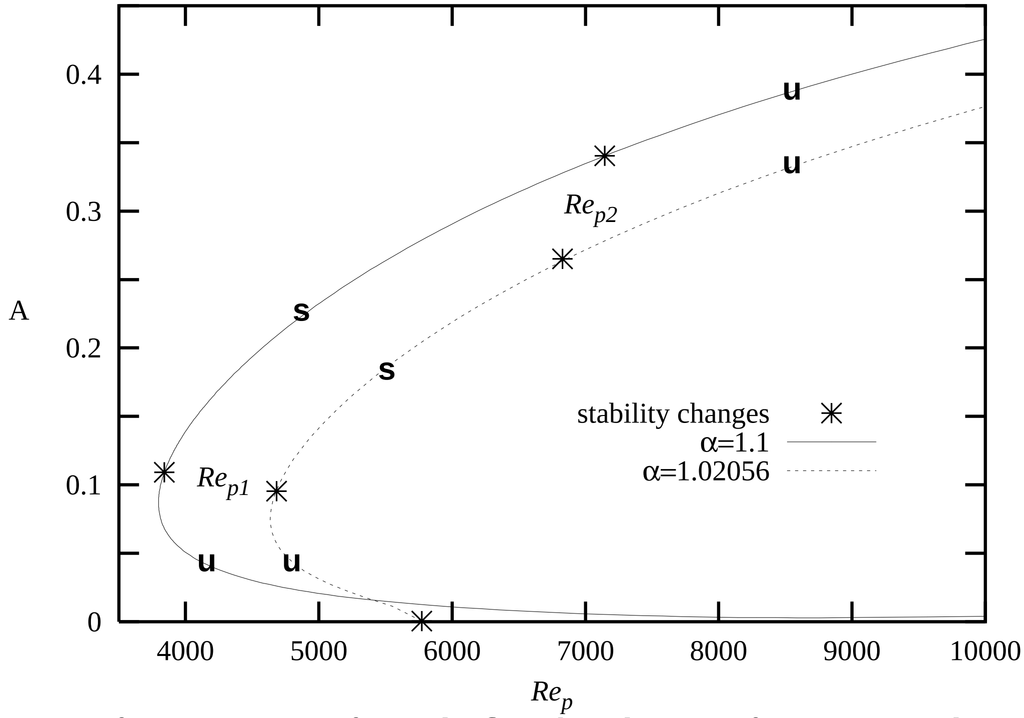

Fig. 1. Bifurcating curves of periodic flows based on Re_p for $\alpha = 1.1$ and $\alpha = 1.02056$. The value of A represents the distance of the periodic flow to the laminar solution. The number of spectral modes retained in the x and y direction are 8 and 70 respectively. The '' on each curve correspond to Hopf bifurcations; two of them are labeled as Re_{p1} and Re_{p2}. They divide the different regions of stability to superharmonic disturbances, which are also labeled in the plot as 's' for "stable" and 'u' for "unstable".*

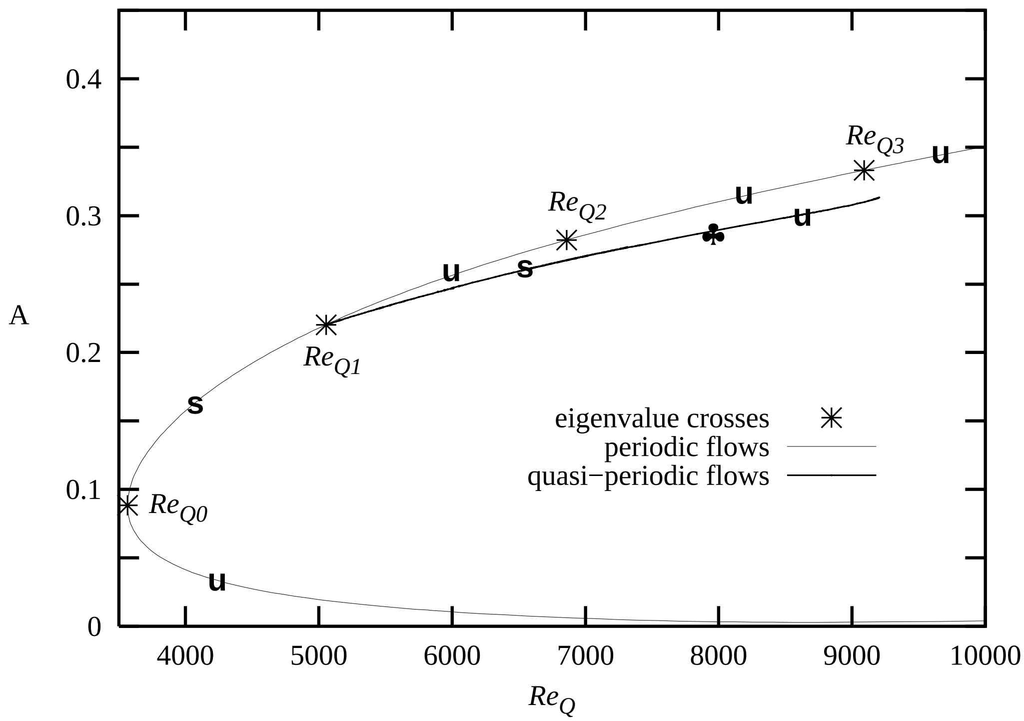

Fig. 2. Analogous of figure 1 based on Re_Q only for $\alpha = 1.1$ but including a branch of quasi-periodic flows. At Re_{Q0} there is no bifurcation whereas three Hopf bifurcations labeled as Re_{Q1} Re_{Q2}, and Re_{Q3} are presented on the upper branch. The symbol ♣ indicates a Hopf bifurcation in the curve of quasi-periodic flows.

$\alpha = 1.02056$		$\alpha = 1.10$		$\alpha = 1.10$	
Re_p	attractor	Re_p	attractor	Re_Q	attractor
4638	laminar	3803	laminar	5264	2-torus
4654	laminar	3816	laminar	5402	2-torus
4680	laminar	3835	laminar	5601	2-torus
6952	2-torus	7268	2-torus	5801	2-torus
7184	2-torus	7615	2-torus	6069	2-torus
7438	2-torus	7991	2-torus	6321	2-torus
7713	2-torus	8398	2-torus	6589	2-torus
8012	2-torus	8839	2-torus	6682	2-torus
8336	2-torus	9316	2-torus	6776	2-torus
8688	2-torus	9832	2-torus		
9067	2-torus	10388	2-torus		
9478	2-torus	10990	2-torus		
9921	2-torus	11638	2-torus		
10398	2-torus				
10912	2-torus				

Table 1. Attractors of the flow to which is connected the unstable manifold of periodic solutions on the upper branch of the amplitude curve. In all cases $N = 8$ and $M = 70$ and $\Delta t = 0.02$.

Unstable invariant manifolds of periodic flows

In our study of the dynamics of plane Poiseuille flow, we are going to analyse the connection between different configurations of the flow, such as laminar, periodic or quasi-periodic. We want to know how the fluid evolves and to which kind of solution it is conducted when it starts on an unstable periodic solution, as the ones shown in figures 1 and 2. We have selected several flows for $\alpha = 1.02056$ and $\alpha = 1.1$, taking for the spatial discretization $N = 8$ and $M = 70$ and for the temporal one $\Delta t = 0.02$. As [3] shows, periodic solutions of Poiseuille flow are stationary in a certain moving frame of reference, and therefore we study their stability by means of linearization. We consider unstable flows that have one real unstable eigenvalue and the remaining ones stable, or a couple of complex conjugate unstable eigenvalues and the remaining ones stable. The lower branch of periodic flows in figures 1 and 2 belong to the first group. In the case of constant pressure, the arc of the upper branch before Re_{p1} and after Re_{p2} for $Re_p < 14000$, correspond to the second group. On the other hand, for Re_Q, only the arc between Re_{Q1} and Re_{Q2} belongs to the second group. For each of those periodic flows $u^p(x, y, t)$, we have studied its unstable manifold and which new state of the fluid they are connected to. By means of the Jacobian matrix (the linearization of the discretized version of (1)) computed to analyze the stability, we can obtain the eigenvector $w \in \mathbb{C}^K$ (K the dimension of the discretized system) associated with the unstable eigenvalue. The perturbed flow $u^p + rw$ for $|r| \ll 1$ is thus a first order approximation of the unstable manifold of u^p, which in turn is an attracting manifold. Using the numerical integrator of (1), we have followed the temporal evolution of $u^p + rw$ until an attracting state is reached. Likewise, in the case that u^p has only one real unstable eigenvalue, we have considered two ways of escaping from u^p namely, taking $r > 0$ or $r < 0$. When there is a couple of complex

$\alpha = 1.02056$		$\alpha = 1.10$		$\alpha = 1.10$	
Re_p	attractor	Re_p	attractor	Re_Q	attractor
4636	laminar	3802	laminar	3658	periodic
4649	laminar	3885	periodic	3694	periodic
4689	laminar	3969	periodic	3816	periodic
4722	laminar	4172	periodic	4020	periodic
4766	periodic	4570	periodic	4559	periodic
4821	periodic	4872	periodic	4611	periodic
4890	periodic	5272	periodic	4814	periodic
4975	periodic	5789	periodic	5101	2-torus
5079	periodic	6397	periodic	5500	2-torus
5205	periodic	6917	periodic	5822	2-torus
5361	periodic	7813	2-torus	6049	2-torus
5554	periodic	8192	2-torus	6499	2-torus
5772	periodic	8642	2-torus	6791	2-torus
		9094	2-torus	7097	2-torus
		9489	2-torus	7359	2-torus
		9589	unknown	7639	2-torus
		10513	2-torus	7995	3-torus
		11078	laminar	8389*	3-torus
		11375	2-torus	8682*	unknown
				9045	unknown
				9363	unknown
				9589	unknown
				9848	unknown
				10139	unknown
				10390	unknown
				10746	unknown
				11096	unknown
				11395	unknown

Table 2. Attractors of the flow to which is connected the unstable manifold of periodic solutions on the lower branch of the amplitude curve. In all cases $N = 8$, $M = 70$ and $\Delta t = 0.02$. The attractors on the table corresponds to one direction of the unstable manifold. On the opposite direction the attractor is the laminar solution, except for a few cases. See the text for details. The temporal evolution is presented in figures 3 and 4 for Re marked with '' in the table.*

conjugate eigenvalues, we have chosen an arbitrary direction in the plane generated by the real and imaginary parts of w.

The different configurations obtained for several values of Re_p, Re_Q and α are summarized in tables 1 and 2. The attractors presented in table 2 are obtained in one direction of the unstable manifold. On the opposite direction the attractor is the laminar solution, except for a few cases. For $Re_Q = 5822$, $\alpha = 1.1$, both directions of the unstable manifold are connected with a 2-torus. For $Re_p = 5772$, $\alpha = 1.02056$, both directions of the unstable manifold are connected with the periodic flow on the upper branch.

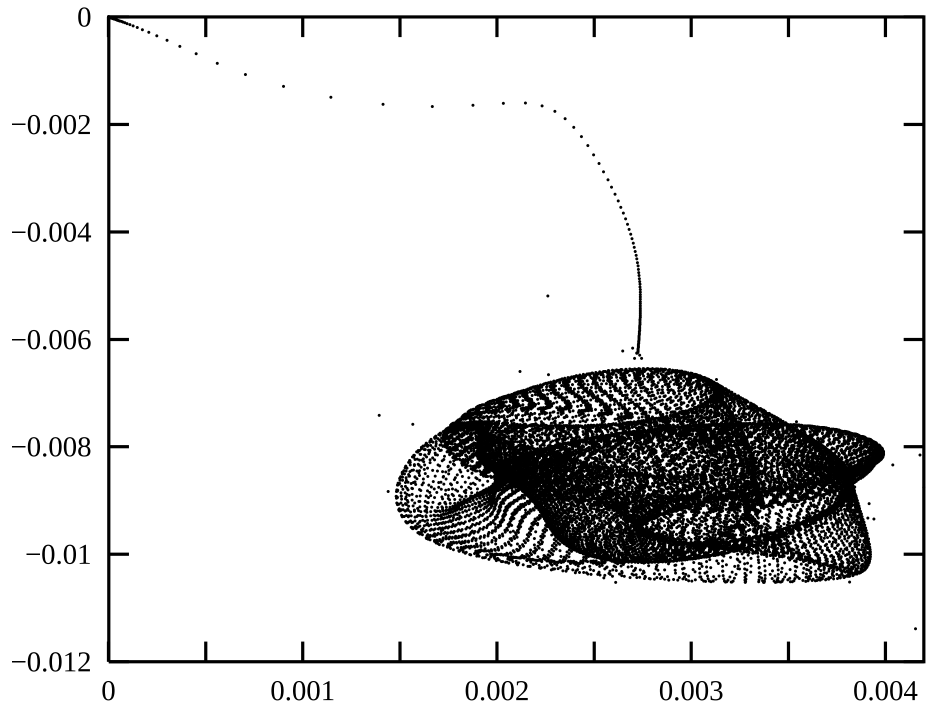

Fig. 3. Flow that starts from the perturbed unstable periodic solution on the lower branch for $Re_Q = 8389$*,* $\alpha = 1.10$*. The flow is first directed to the unstable periodic flow on the upper branch and then attracted by a* 3*-torus. The integration time on the figure is about* $322{,}000$ *time units.*

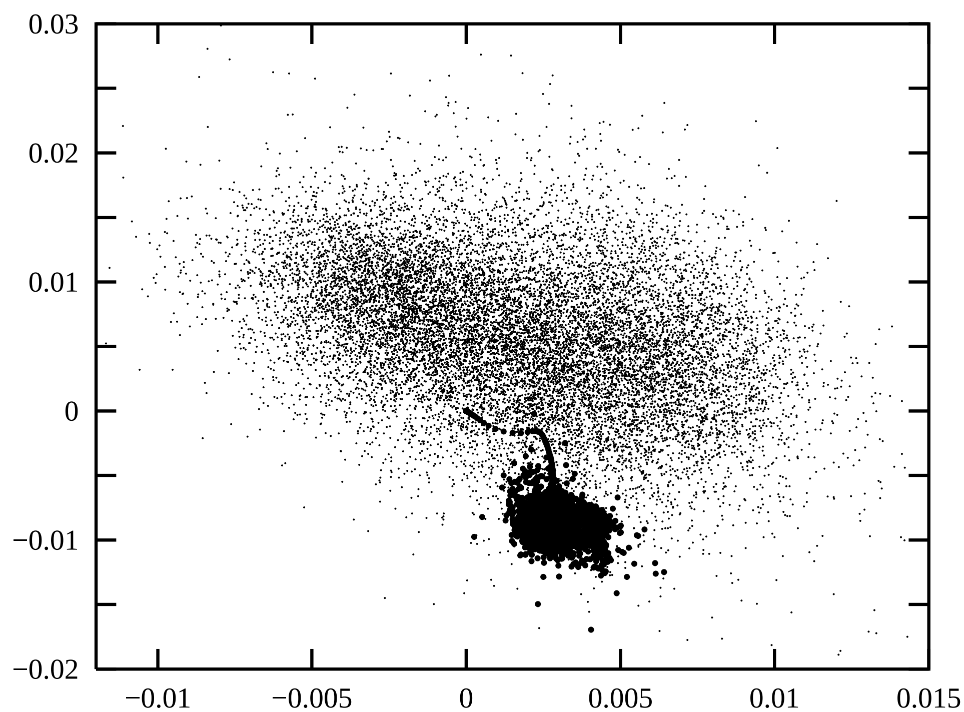

Fig. 4. Flow that starts from the perturbed unstable periodic solution on the lower branch for $Re_Q = 8682$*,* $\alpha = 1.10$*. The flow is attracted by a strange set plotted in bigger dots, which is unstable and finally drives the fluid to another strange set. The integration time on the figure is about* $245{,}000$ *time units.*

Re_Q	attractor	Re_Q	attractor	Re_Q	attractor
7953	3-torus	8322^*	3-torus	8894	possible 3-torus
7975	3-torus	8486	3-torus	9005^*	possible 3-torus
8043	3-torus	8623	3-torus	9096	unknown
8157	3-torus	8767	3-torus	9204	unknown
8278	3-torus				

Table 3. Attractors of the flow to which is connected the unstable manifold of quasi-periodic solutions. In all cases $N = 8$, $M = 70$, $\alpha = 1.1$ and $\Delta t = 0.02$. The temporal evolution of the flow until the attracting solution is reached is presented in figures 5 and 6 for Re marked with '' in the table.*

For the case of Re_p, $\alpha = 1.02056$, the lower branch is connected with the laminar flow for $Re_p \lesssim 4722$, and with a periodic solution for $4766 \lesssim Re_p \lesssim 5772$. For the case of Re_p, $\alpha = 1.1$, the connection of the lower branch is with the laminar flow for $Re_p \lesssim 3802$, with a periodic flow for $3885 \lesssim Re_p \lesssim Re_{p2}$, with a 2-torus for $Re_{p2} \lesssim Re_p \lesssim 9500$, and with different configurations for $Re_p \gtrsim 9500$. For Re_Q, $\alpha = 1.1$, the lower branch is connected with a periodic solution for $Re_Q \leqslant Re_{Q1}$, with a 2-torus for $Re_{Q1} \leqslant Re_Q \lesssim 7950$, with a 3-torus for $7950 \lesssim Re_Q \lesssim 8500$, and with unknown sets for $Re_Q \gtrsim 8500$. In this case, for $Re_Q \geqslant Re_{Q1}$ the perturbed unstable periodic flow is first connected with the periodic solution on the upper branch and then is directed to the final attractor. The upper branch is connected with the laminar flow for $Re_p \leqslant Re_{p1}$, and with a 2-torus for $Re_{p2} \leqslant Re_p \leqslant Re_{p3}$, for $\alpha = 1.02056$ and, $\alpha = 1.1$, being Re_{p3} the next Hopf bifurcation after Re_{p2}. For the case of Re_Q, $\alpha = 1.1$, the upper branch is also connected with a 2-torus for $Re_{Q1} \leqslant Re_Q \leqslant Re_{Q2}$. In figures 3 and 4 we present the evolution of the perturbed periodic flow. On those figures we plot the projection of the discrete velocity on the plane of 2 coordinates (956 and 210 out of 1156, to be precise) when the flow crosses an appropriate Poincaré section (see [1] for details) Σ_1. For instance, on Σ_1 the evolution of a stable periodic flow is represented by a single constant point on those projections and the laminar flow by coordinates $(0, 0)$.

Unstable invariant manifolds of quasi-periodic flows

In the case of constant flux the bifurcation diagram of periodic flows is qualitatively different to that of constant pressure, as is shown in figures 1 and 2. For Re_Q and $\alpha = 1.1$ there is a change of stability at the minimum Reynolds Re_{Q0} of the curve of amplitudes, but no new bifurcations are born there. The first Hopf bifurcation occurs at the point labeled Re_{Q1} in figure 2.

The quasi-periodic solutions found from Re_{Q1} are stable for $Re_{Q1} < Re_Q \lesssim 7950$. At $Re_Q \approx 7950$ the branch of quasi-periodic solutions loses stability to give rise to a family of attracting tori of 3 basic frequencies at a new Hopf bifurcation.

In table 3 we show the connections of the unstable manifold corresponding to the unstable 2-tori for $Re_Q \gtrsim 7950$. The procedure follows the same lines as for the case of periodic flows described previously. For each unstable 2-torus u^q, we approximate the linear part (this is computed in parallel) of the Poincaré map P_c defined on Σ_1 (quasi-periodic flows

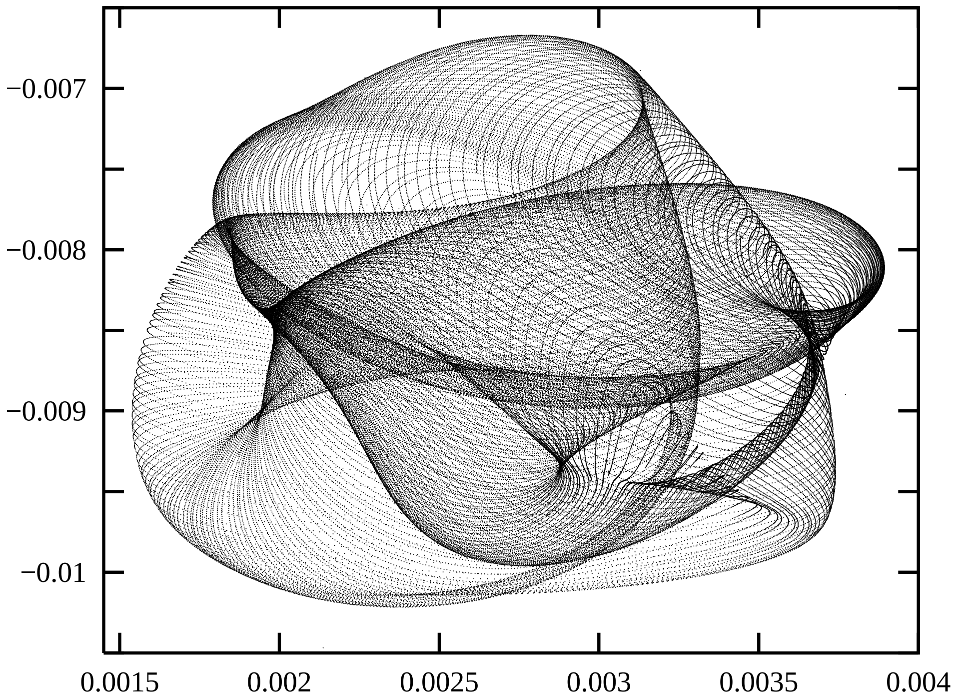

Fig. 5. Evolution of the perturbed 2*-torus for* $Re_Q = 8322$*, which is attracted by a nearly resonant* 3*-torus, as can be observed. The total integration time is of the order of* $2{,}108{,}000$ *time units.*

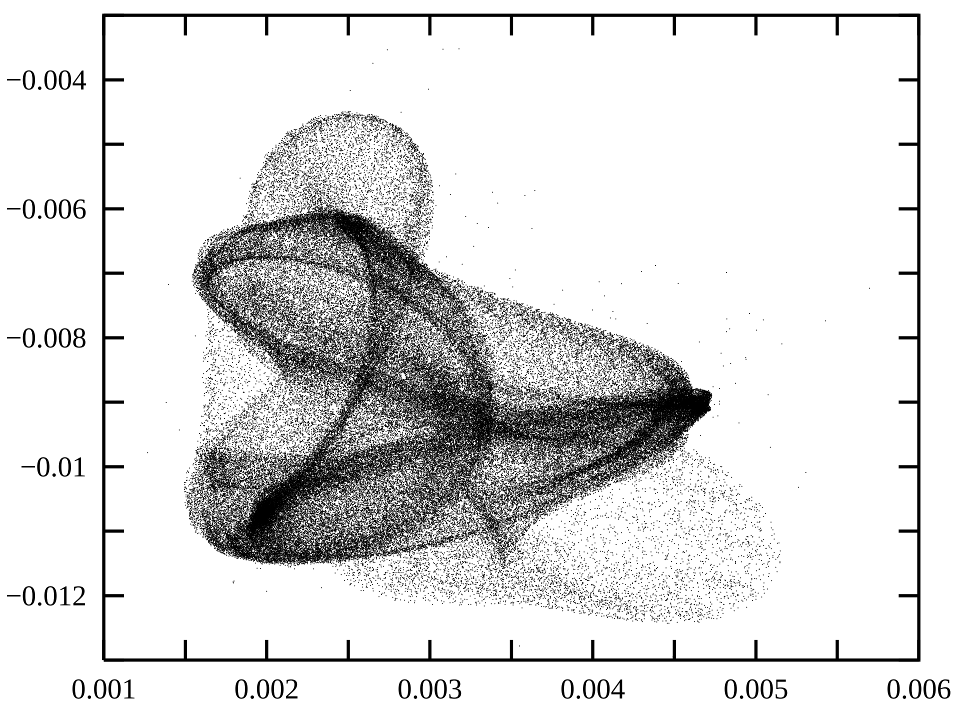

Fig. 6. Evolution of the perturbed 2*-torus for* $Re_Q = 9005$*, which is attracted by a set that reminds a* 3*-torus. The total integration time is about* $2{,}114{,}000$ *time units.*

are proved in [3] to be periodic in an appropriate moving frame and thus fixed points of P_c), by means of extrapolated finite differences. Then we perturb u^q in the direction of the most unstable eigenvectors of the linear part of P_c, associated to two complex conjugate eigenvalues of modulus greater than 1. We follow the temporal evolution of this perturbed flow until an attracting state is reached. For $Re_Q \lesssim 9000$ the attracting flow seems to be a 3-torus, but for greater Re_Q the solution becomes apparently disordered. In figures 5 and 6 we show the temporal evolution for the perturbed quasi-periodic flows for $Re_Q = 8322$ and $Re_Q = 9005$. The attracting solution for $Re_Q = 8322$ is a quasi-periodic flow with 3 basic frequencies close to resonant. In the case of $Re_Q = 9005$, the final attractor observed in the Poincaré section resembles a possible 3-torus.

References

[1] Pablo S. Casas. *Numerical study of Hopf bifurcations in the two-dimensional plane Poiseuille flow*. PhD thesis, Universidad Politécnica de Cataluña, September 2002. http://www-ma1.upc.es/˜casas/research.html.

[2] Th. Herbert. Periodic secondary motions in a plane channel. In *Proc. 5th Intl. Conf. on Numerical Methods in Fluid Dynamics*, volume 59 of *Lecture Notes in Physics*, pages 235–240. Springer, 1976.

[3] D. Rand. Dynamics and symmetry predictions for modulated waves in rotating fluids. *Arch. Rat. Mech. Anal.*, 79:1–37, 1982.

[4] B. L. Rozhdestvensky and I. N. Simakin. Secondary flows in a plane channel: their relationship and comparison with turbulent flows. *J. Fluid Mech.*, 147:261–289, 1984.

[5] Israel Soibelman and Daniel I. Meiron. Finite-amplitude bifurcations in plane Poiseuille flow: two-dimensional Hopf bifurcation. *J. Fluid Mech.*, 229:389–416, 1991.

Acknowledgements

This research has been partially supported by funds from the Departamento de Matemática Aplicada I (Universidad Politécnica de Cataluña), the Spanish CICYT grant BFM2000–0623, the Catalan CIRIT grant 2001SGR–70, and DURSI.

1. Departamento de Matemática Aplicada I. Universidad Politécnica de Cataluña.
Diagonal, 647; 08028 Barcelona. Spain.
e-mail: `pablo@casas.upc.es`

2. Departamento de Matemática Aplicada y Análisis. Universidad de Barcelona.
Gran Via, 585; 08007 Barcelona. Spain.
e-mail: `angel@maia.ub.es`